

Viscoelastic Properties of a Resin Commonly Used in the Single Fiber Fragmentation Test

Donald Hunston*, Gale Holmes, Richard Peterson
National Institutes of Standards and Technology
Polymers Division
Gaithersburg, MD 20899

ABSTRACT: The fiber-matrix interface can play an important role in the performance of a composite, and consequently, it has been the subject of considerable study. One of the experiments often used to characterize the strength or quality of the interface is the single-fiber fragmentation test. The models used to analyze the data from this test involve a number of assumptions, one of which is the constitutive behavior of the matrix resin. To evaluate this assumption, a fragmentation apparatus was modified to include a load cell so both stress and strain could be measured during the experiment. Surprisingly, the results show that not only is the behavior viscoelastic, but virtually all of the fragmentation takes place in a range where the response is non-linear. To characterize this behavior, single-step, stress-relaxation experiments were conducted on a resin system often used in such tests. The results indicate that a simple power law model with strain-dependent parameters could describe the behavior over a very wide range of conditions. By using this characterization and the strain history, a crude fit to the actual loading curve in a fragmentation tests could be obtained. In order to achieve quantitative agreement, however, a modified power law model was required. Such a relationship was shown to describe the loading curve for two quite different loading procedures.

INTRODUCTION

There has been growing interest over the last 15 years in the fiber-matrix interface because researchers have become increasingly aware of the important role it can play in composite performance (1-4). One of the parameters often determined is τ . Usually termed the interfacial shear strength, but it is probably more accurately described as a parameter related to the ability of the interface region to transfer stress between the fiber and the matrix. Numerous test methods have been used to measure τ or a similar parameter, but probably the most common is the single fiber fragmentation (SFF) test (5, 6). The work in this paper focuses on this test but is

This paper was originally presented at the *Proceedings of the 13th Annual Technical Conference on Composites Materials*, September 21-23, 1998, Baltimore, MD. This paper is declared a work of the U.S. Government and is not subject to copyright protection in the United States.

* Author to whom correspondence should be addressed.

Reprinted from Journal of Reinforced Plastics and Composites, Vol. 18, No. 18/1999

relevant to other interface measurement methods as well.

In the SFF test, a dogbone of resin is fabricated with a single fiber along the long axis of the sample. The resin should be transparent^a and have a higher extension to failure than the fiber. The dogbone is loaded in tension, and some of this load is transferred into the fiber through the interface. As the strain increases, the load in the fiber eventually causes the fiber to break. Further loading produces additional breaks in the fiber until the fragments become so small that it is no longer possible to transfer sufficient load into the fiber fragments to cause them to reach their failure strains. This point is called saturation. The lengths of the fragments at saturation are measured, and these data are used to calculate τ based on an appropriate model.

A variety of such models have been developed, and each has a slightly different set of assumptions. An important example is the constitutive behavior used for the resin. The earliest model assumed the resin to be perfectly plastic, and this produced a final equation which does not contain the matrix modulus (8). This led many researchers to conclude that the matrix properties were not important in the calculation of τ . Although this is now known to be a poor assumption, most experiments hold the matrix constant and alter the fiber surface treatment so there are no changes in the matrix behavior to affect the comparative results. Consequently, the relative values are directly useable.

The second generation of models, often based on old stress analyses (9), assumed linear elastic behavior for the resin, and under these conditions, the matrix modulus usually does appear in the final equations. Consequently, changes in modulus have a direct effect on the evaluation of τ and need to be considered. Although this represents an important advance, there is still considerable concern in the community that linear elastic behavior may be a significant over simplification. Numerous experimental studies and model development efforts have explored this area in recent years (10-18). They generally conclude that a more sophisticated constitutive equation is needed. The purpose of this paper is to test this idea by examining the stress-strain behavior of a sample during a fragmentation experiment. Based on this result, tests were performed to characterize the basic non-linear viscoelastic behavior of the resin. These results were then compared with fragmentation data, and a modified model was developed to describe the material's behavior in this experiment.

EXPERIMENTAL STUDIES^b

MATERIALS

The resin system studied in this work, diglycidyl ether of bisphenol A (Epon 828 from Shell Chemical Co.) cured with meta-phenylene diamine (Fluka Chemical Company), is one of the most commonly used polymers for the SFF test. Most samples did not contain a fiber so the resin behavior itself was obtained. When fibers were used, they were E-glass (Owens Corning) with an commercial, epoxy-compatible sizing. Details of the sample preparation procedure are given

^aTechniques for non-transparent samples have been developed but are not widely used (5, 7).

^bCertain commercial materials and equipment are identified in this paper in order to specify adequately the experimental procedure. In no case does such identification imply recommendation or endorsement by the National Institute of Standards and Technology, nor does it imply necessarily that the items are the best available for the purpose.

elsewhere (5).

FRAGMENTATION TEST

In the SFF tests performed at the National Institute of Standard and Technology (NIST), the sample is loaded in a jig mounted on a microscope, Figure 1. One of the grips in the jig is moveable and attached to a threaded rod. A knob at the other end of the rod is turned to load the sample. The loading is done in a series of small steps. Each step is a nominal strain increase of 0.001, but the nature of the apparatus means that this is only approximate. After each loading increment, there is a pause before looking for fiber breaks since experiments have shown that new

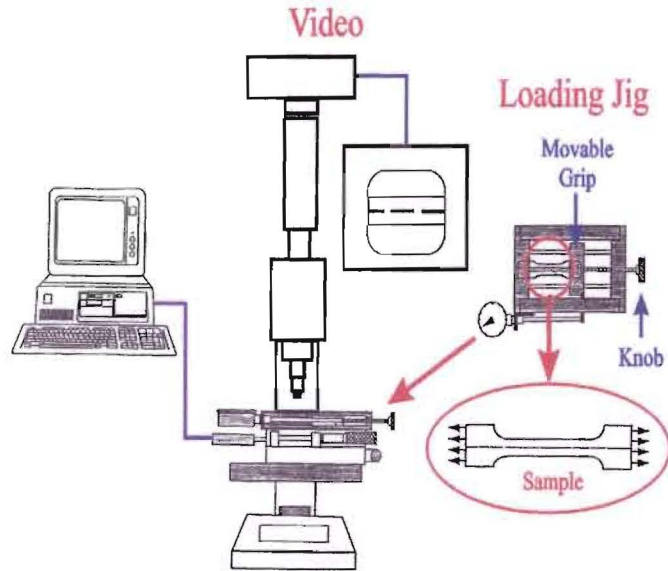


Figure 1: Diagram of fragmentation apparatus.

breaks can occur for a short time after the strain step. Although this behavior is not fully understood, tests have indicated that a pause of 10 min. allows the experiment to produce reproducible results (17,19). In the standard test procedure used at NIST, the sample is loaded and just before the end of each 10 min pause scanned for breaks in the gage section (length between 1.0 cm and 1.5 cm). The scan is done by translating the loading jig beneath the microscope. The microscope image is picked up by a video camera and displayed on a monitor so the breaks can easily be counted. In addition to counting breaks, the strain in the sample is measured before and after each step. To measure the strain, two marks are placed on the sample surface at the ends of the gage length. The jig is moved beneath the microscope until one mark is lined up with a cross-hair on the monitor. The movement of the jig is measured by a displacement transducer (LVDT), and when a button is pushed, the current location of the jig is recorded into a computer. By doing this for both marks, the strain can be measured. The fragmentation test repeats this procedure which causes the sample to be loaded in a series of strain steps at 10 min. time intervals. For the early steps, few if any fiber breaks are observed. At intermediate strains, each step produces new breaks. Finally, a point is reached where no new breaks are found for three consecutive loading steps. This is taken as the saturation point. Once saturation is achieved, the break locations are determined through out the gauge length using the same procedure employed to locate the strain marks. These data are stored in a computer file for later analysis.

In addition to this standard test procedure, many specimens at NIST have been measured using a more detailed process. In this case, the fiber break locations are monitored for each step after the 10 min. pause. Since this process takes some time, the delay between each strain step increases as the number of breaks gets larger.

In order to visualize the fiber break pattern, particularly with the more detailed measurement process, a program was written to display the data stored in the computer. Figure 2 (top) shows typical output from the program. The fiber is represented by two closely spaced horizontal lines. Twelve different strain steps are included in the figure, one above the other. The breaks are

indicated by the vertical lines through the fiber. When there is a region of debonding near a fiber break, each end of debonded area is marked with a separate vertical line, these lines are connected at the bottom, and a short line extends down from the connecting lines to mark the approximate position of the break. To better visualize the break pattern that develops, each new fiber is translated and scaled and so that the corresponding breaks align vertically. The scaling factors provide an alternate way to determine the relative strain once a number of breaks are present. The strain and number of breaks are indicated along the right side of Figure 2. To better view the details of the fragmentation pattern, the program can provide an expanded view of any portion of the fiber. This is illustrated in Figure 2 (bottom) which shows a magnified section from the top figure. The program also outputs a file containing the number of breaks as a function of strain. This information can be plotted as shown in Figure 3. Such a plot provides a good way to verify that saturation has been achieved since saturation should produce a plateau such as that seen in Figure 3.

For the experiments conducted in the present work three different stain histories were measured. The first simulates the standard fragmentation test and has equally spaced loading steps separated by 10 min. The second history examined here uses this same procedure but with a 1 h pause between each loading step. In the third history, the pauses between loading steps increase with total strain in a way that simulates the detailed measurement process for conducting the fragmentation test.

Fragmentation Break Pattern

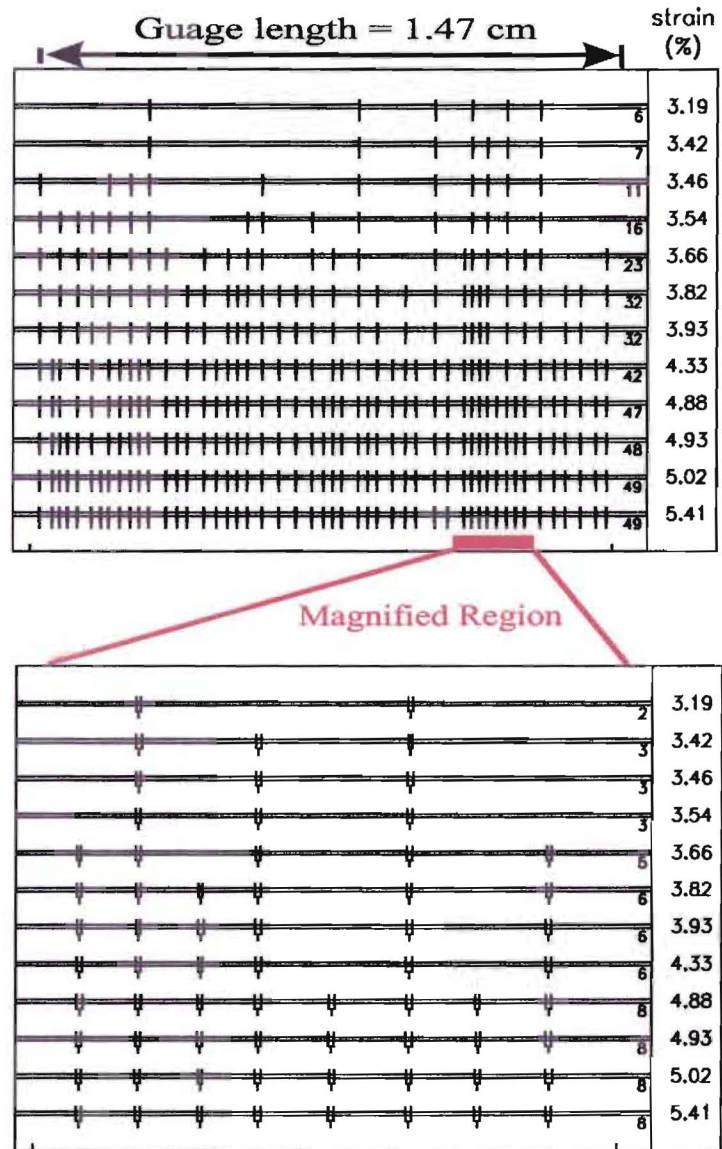


Figure 2: Fragmentation pattern displayed by computer program. Top plot is for full gauge length while bottom plot is expanded portion of top figure. Along the right side of each plot are numbers indicating the strain (%) and the total breaks in the section shown.

LOAD MEASUREMENT

To examine the constitutive behavior of the resin, the fragmentation apparatus was modified to add a load cell. The stationary grip was attached to the load jig through either a 2.2 KN or a 1.1 KN load cell (Cooper Instruments, LPM 530). The load cell is connected through a transducer conditioner/digitizer (Cooper Instruments, DA101/AED9001A) to the serial port of the computer. The data acquisition software was modified so that the load was continuously recorded during the experiment except for the period when the fragments are being measured. Although the system is capable of much higher data acquisition rates, the monitoring was usually set for two load measurements per second since the experiments were slow. To minimize the amount of data stored, a sensitivity level was set in the program, and only changes outside this level were saved. The results were continuously plotted on the computer screen so the behavior could be monitored in real time.

BASIC RESIN BEHAVIOR

To compliment the measurements made during the fragmentation experiment, the resin's basic viscoelastic behavior was determined. Since the SFF test involves step-strain loading, single-step stress relaxation measurements were used. For large strains, the SFF apparatus was employed on dogbone samples without fibers. This worked well at strains above 0.8 %. Strains below that level were difficult to apply because they required small rotations of the knob attached to the threaded rod. As a result, a second apparatus was used to add small strain data. Grips identical to those for the SFF apparatus were constructed for a Dynastat® testing machine. This apparatus is designed to measure linear viscoelastic behavior and is therefore well suited to small strain tests. Unfortunately, the measurement of grip displacement was found to be inadequate for calculation of the strain so an extensometer was used to this parameter. The time required for manual loading of the sample in the SFF apparatus was approximately 1 s which means that stress relaxation data were obtained between 10 s and 10⁵ s (about 27 h). The Dynastat allowed loading in 10 ms or less so data from 0.1 s to 10⁵ s could be measured.

To assure compatibility of data from the two measurements, a cross-calibration was conducted. The extensometer used to measure strain on the Dynastat was attached to the SFF apparatus, and the agreement between strain values determined from the extensometer and from displacement measurements of the marks on the specimen was well within the experimental error for the latter (standard uncertainty was 0.0008 mm for the extensometer and 0.0016 mm for the

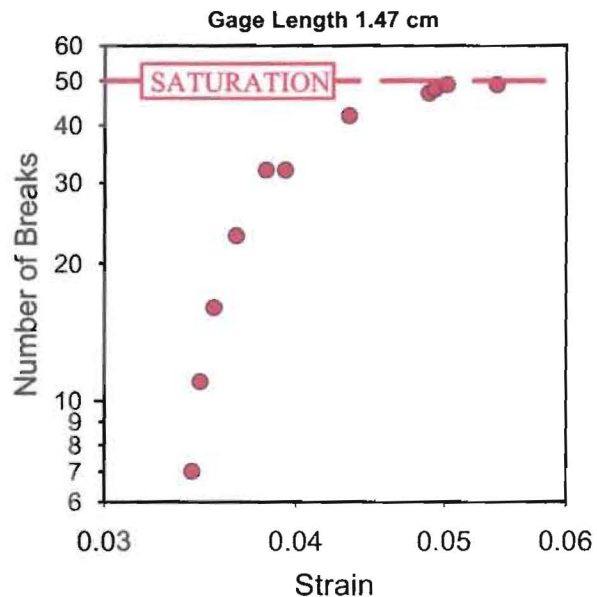


Figure 3: Fiber breaks as a function of strain from data in Figure 2.

displacement technique). The load cell from the SFF apparatus was mounted in the Dynastat, and the readings were compared over a range of loads. The SFF cell gave values that were 1.03 times those from the Dynastat. Since the SFF load cell had been directly calibrated against standard weights, a corresponding correction was introduced into the Dynastat data on the assumption that the difference was due to a drift in the Dynastat calibration. Finally, a number of stress relaxation experiments were run for comparison. The Dynastat's load cell limits the experiments to strains below 0.8 %, but in the range from 0.5 % to 0.8 %, tests were conducted with both methods. The agreement was well within the experimental uncertainty for the modulus determination (standard uncertainty was 0.13 GPa).

LOAD FRAME STIFFNESS

With a stress relaxation experiment, the machine stiffness can be important. As the stress decreases during the test, the load frame can expand slightly. This produces an increase in the strain in the sample. Thus the experiment is not a constant strain test. The load frame on test machines like the Dynastat are designed to be very stiff so this effect is negligible. Measurements with the extensometer confirm this since no change in strain can be detected. Since the SFF test is not designed for such experiments, stiffness is a concern. In the usual fragmentation experiment, there is no problem because the strain is changed and measured at each step while the amount of relaxation that occurs between each step is small. When the SFF apparatus is used in characterization experiments, however, a single step is applied and held for up to 1 day. Significant relaxation can occur in that time. To examine this question, the strain was measured just after the strain was applied and at the end of the experiments. At the lower strains where the amount of relaxation (decrease in load) was only moderate, little or no change in strain was detected. At the highest loads, however, a small increase in strain was found. This could be used to estimate the stiffness of the apparatus, and the results indicate that the grips extend by about 0.0004 mm for each 1 N drop in load. This means that a sample strained by 5 % initially will have a strain of 5.2 % at the completion of the test. This represents a deviation for pure stress relaxation. Since this difference is small, it was felt that simply correcting the data for this slight change in strain during the experiment would be sufficient to provide meaningful results.

RESULTS

Figure 4 shows an example of a load vs time curve for a sample without a fiber. Each strain-step was followed by a 1 hour pause. It is difficult to judge the behavior when the data are plotted in this way so several comparison curves were added for model material behavior. The first assumes linear elastic behavior and utilizes the early steps to estimate the modulus. Although the fit at low strains is good, the curves diverge significantly at higher strains. This is not really surprising since significant relaxation of the load can be seen in the measured curve during the constant strain regions between steps. Consequently, a second comparison is made using a linear viscoelastic model. Again, the low strain data were used to estimate the viscoelastic parameters. A simple power law model was chosen to describe the behavior based on data that will be presented later. As with the elastic model, agreement at low strains is good, but at high strains the introduction of viscoelasticity improves the prediction only slightly. Although this sample did not contain a fiber, it is possible to estimate where the breaks would occur based on measurements with other samples.

The approximate position where the first break would occur and where the saturation point would be reached are indicated in the figure.

These results suggest several things. First, the linear elastic and linear viscoelastic models are inadequate to describe the behavior. Second, all of the breaks occur in the region where the model predictions fail. Consequently, a non-linear viscoelastic relationship is clearly required. This result helped motivate the subsequent work to characterize the resin's behavior.

Figure 5 shows typical curves from the stress relaxation experiments. Below a strain of about 0.6 % the behavior is linear viscoelastic. At higher strains, the modulus is lower and the time dependence is stronger. Over the entire range, however, the curves are approximately linear on a log-log plot. As a result, a simple power law model with a strain dependent coefficient and exponent can provide a very good description of the behavior. The tensile modulus, $E(\epsilon, t)$, is related to the time, t , by

$$E(\epsilon, t) = E_{100}(\epsilon) \left[\frac{t}{100} \right]^{\theta(\epsilon)} \tag{1}$$

The 100 second modulus, $E_{100}(\epsilon)$, could be described as

$$E_{100}(\epsilon) = \begin{cases} 3.27 & (\epsilon \leq 0.005) \\ 3.52 e^{-16.06 \epsilon} & (\epsilon > 0.005) \end{cases} \tag{2}$$

while the power law exponent, $\theta(\epsilon)$, is given by

$$\theta(\epsilon) = \begin{cases} 0.008 & (\epsilon \leq 0.005) \\ 0.1159 (\epsilon - 0.00427)^{0.370} & (\epsilon > 0.005) \end{cases} \tag{3}$$

Equation (2) combines a region of linear behavior ($\epsilon < 0.005$) with a region where there is an exponential dependence on strain. An exponential dependence on strain has been used by a number

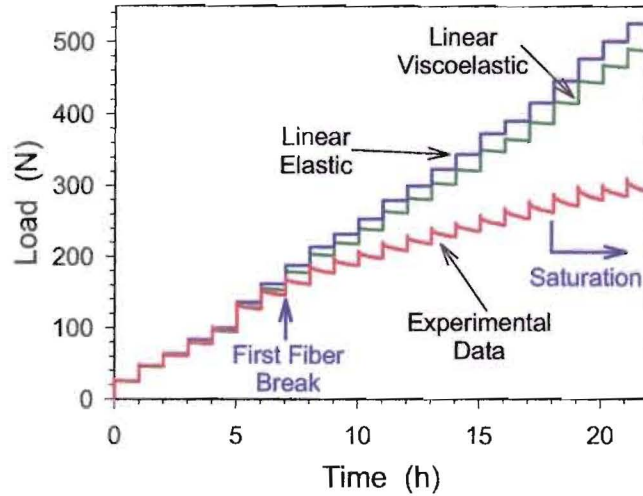


Figure 4: Fragmentation experiment loading curves and predictions for linear elastic and viscoelastic models. Standard uncertainty in the load measurement is 2 N.

of authors; for example, Matsuoka et al. (20) employed a similar model to describe the behavior of polycarbonate. Equation (3), on the other hand, is simply a convenient equation designed to fit the data.

Based on these results and the measured strain history, an effort was made to predict the fragmentation loading curve, which is a multiple step experiment. A modified Boltzmann Superposition Principle was used with the non-linear viscoelastic modulus, eqs. (1-3) to calculate the load as a function of time, $L(t)$

$$L(t) = A_s \sigma(\epsilon, t) = A_s \sum_{i=1}^N \left[\sigma(\epsilon_p, t-t_i) - \sigma(\epsilon_{i-1}, t-t_i) \right] \quad (4)$$

where A_s is the cross-sectional area of the sample, and $\sigma(\epsilon, t)$ is the stress. As noted by Christensen, there is no theoretical basis for this expression (21), but it has been shown to be useful for a number of cases (22, 23).

Figure 6 shows the results of this prediction for the experiment in Figure 4 (curve marked Prediction from Single Step Data). This model is clearly an improvement over the linear models (see Figure 4). At the saturation point (about 18 h), the new prediction is relatively lower than the

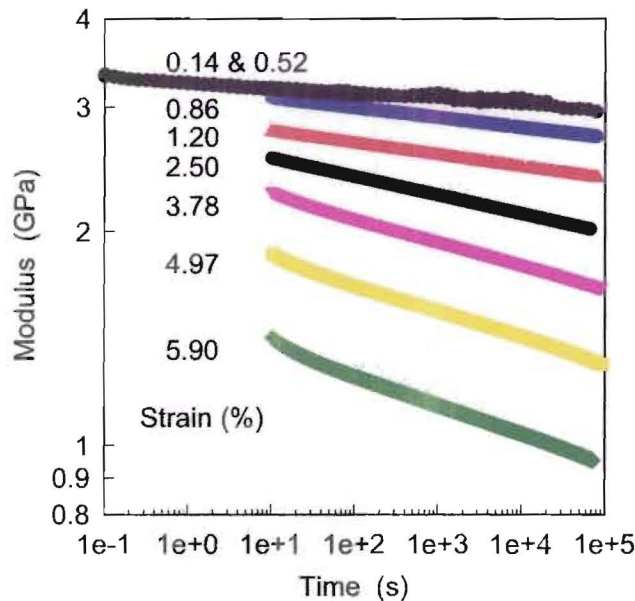


Figure 5: Results from stress relaxation experiments. Data for two lowest strains were obtained with Dynatsat while the remaining results came from experiments using the fragmentation apparatus. Standard uncertainty in the modulus data is 0.13 GPa.

experimental value by only 15 %. This compares to the linear viscoelastic and elastic predictions which exceed the experimental value by factors of 1.4 and 1.5, respectively. This new model accounts for the non-linearity which is very important but seems to underestimate the time dependence relaxation between steps and overestimate the non-linearity at high strains.

In order to account for the differences that still exist between the experiment and model, a variety of empirical modifications of the power law relationships were investigated. Details of this are published elsewhere (13), but the best result was obtained with a bi-exponential damping function. A similar expression was used by Osaki and Laun to describe polyethylene (24, 25). This relationship is given by

$$E(\epsilon, \dot{\epsilon}_{ave}, t) = E_o \left(1 + \frac{t}{\tau} \right)^{-\kappa(\dot{\epsilon}_{ave})} \left[\begin{array}{l} f_1 e^{-C_1 \epsilon} \left(1 + \frac{t}{\tau} \right)^{-\theta_1(\epsilon)} + \\ (1-f_1) e^{-C_2 \epsilon} \left(1 + \frac{t}{\tau} \right)^{-\theta_2(\epsilon)} \end{array} \right] \quad (5)$$

This relation has 7 parameters: f_1 , C_1 , C_2 , and E_o are constants, θ_1 and θ_2 are functions of strain, while κ is independent of strain but does vary with loading history. This dependence on loading history is characterized by the average strain rate, $\dot{\epsilon}_{ave}$, which is the total strain at the end of the experiment divided by the total loading time.

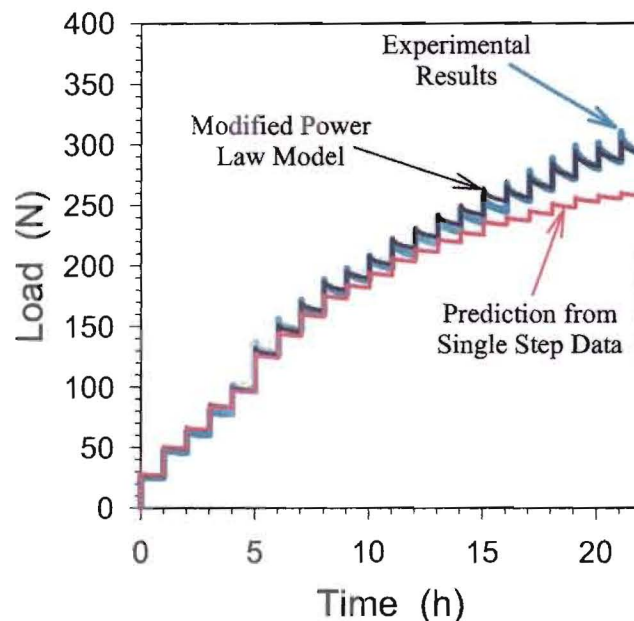


Figure 6: Fragmentation experiment loading curve and model predictions. Standard uncertainty in the load measurement is 2 N.

The fit of eq. (5) to the data is shown in Figure 6 (curve marked Modified Power Law Model). Although the model is empirical, it accurately reproduces all of the features in the experimental curve. In this particular experiment, each step was held for 1 h before the next step is initiated. A similar curve with 10 minute holds between steps has also been generated, and the model provides an equally good fit to those data.

CONCLUSIONS

A load cell was added to a single fiber fragmentation apparatus to investigate the constitutive behavior of the matrix resin. The results show that the polymer exhibits strong non-linear viscoelasticity in the range where fragmentation occurs. Basic characterization of the resin using single-step stress-relaxation experiments gave results that could be described over wide ranges of time and strain by a power law model. Prediction of the loading curve in the fragmentation experiment from the basic characterization results gave a curve that was within 15% of the experimental result through the saturation point. A modified model with a bi-exponential damping function, however, gave excellent agreement with the measured data.

REFERENCES

1. McKenna, G. B., "Interlaminar Effects in Fiber-Reinforced Plastics-A Review," *Polymer Plast. Tech. Eng.* **5(1)**, 23-53 (1975).
2. Madukar, M. S., and Drzal, L. T., "Fiber-Matrix Adhesion and its Effects on Composite Mechanical Properties: I. In Plane and Interlaminar Shear Behavior of Graphite/Epoxy Composites," *J. Compos. Mater.* **25**, 932-956 (1991).
3. Madukar, M. S., and Drzal, L. T., "Fiber-Matrix Adhesion and its Effects on Composite Mechanical Properties: II. Longitudinal (0°) and Transverse (90°) Tensile and Flexure Behavior of Graphite/Epoxy Composites," *J. Compos. Mater.* **25**, 957-991 (1991).
4. Schultheisz, C. R., McDonough, W. G., Kondagunta, S., Schutte, C. L., Macturk, K. S., McAuliffe, M., and Hunston, D. L., "Effects of Moisture on E-Glass/Epoxy Interfacial and Fiber Strengths," in ASTM Symposium on Composite Materials: Testing and Design, ASTM STP-1242 (ASTM, West Conshohocken, PA, in press).
5. Drzal, L. T., and Herrera-Franco, P. J., "Composite Fiber-Matrix Bond Tests," pp. 391-405 in *Engineered Materials Handbook: Adhesive and Sealants*, Vol. 3 (ASM International, Metals Park, Ohio, 1990).
6. Herrera-Franco, P., Wu, W. L., Drzal, L. T., Hunston, D. L., "Comparison of Methods to Assess Fiber-Matrix Interface Strength, p. 21-23 in Proc. of Adhesion Society Meeting. (Adhesion Society, Blacksburg, 1991).

7. Netravali, A. N., Li, Z. F., Sachse, W., and Wu., H. F., "Determination of Fiber/Matrix Interfacial Shear Strength by an Acoustic Emission Technique," *J. Mat. Sci.* **26**, 6631-6638 (1991).
8. Kelly, A., and Tyson, W. R., *J. Mech. Phys. Solids* **13**, 329 (1965).
9. Cox, H. L., "The Elasticity and Strength of Paper and Other Fibrous Materials," *British Journal of Applied Physics* **3**, 72-79 (1952).
10. Gent, A. N., Chang, Y. W., Nardin, M., and Schultz, "Mechanics of Fibre Fragmentation," *J. Mat. Sci.* **31**, 1707-1714 (1996).
11. Hui, C. Y. , Pheonix, S. L., and Kogan, L., "Analysis of Fragmentation in the Single Filament Composite: Role of Fiber Strength Distribution and Excluded Zone Models," *J. Mech. Phys. Solids* **44(10)**, 1715-1737 (1996).
12. Herrera-Franco, P. J., Rao, V., Drzal, L. T., and Chiang, M. Y. M., "Bond Strength Measurement in Composites--Analysis of Experimental Techniques," *Composites Eng.* **2(1)**, 31-45 (1992).
13. Holmes, G. A., Peterson, R. C., and Hunston, D. L., "Modeling of Multi-Step Nonlinear Stress Relaxation in DGEBA/m-PDA Epoxy Resins," to be published.
14. Melanitis, N. Galiotis, C., Tetlow, P. L., and Davis, C. K., "Monitoring the Micromechanics of Reinforcement in Carbon Fibre/Epoxy Resin Systems," *J. Mat. Sci.* **28**, 1648-1654 (1993).
15. Tripathi, D., Ali, S., Lopatananon, N., Jones, f. R., "Technological Solutions to the Testing and Data Analysis of Single Fibre Fragmentation Test," to be published.
16. Di Asclmo, A. Accorsi, M. L., and DiBenedetto, A. T., "The Effect of an Interphase on the Stress and Energy Distribution in the Embedded Single Fibre Test," *Compos. Sci. & Tech.* **44**, 215-225 (1992).
17. Monette, L., Anderson, M. P., and Grest, G. S., "The Meaning of the Critical Length Concept in Composites: Study of Matrix Viscosity and Strain Rate on the Average Fiber Fragmentation Length in Short-Fiber Polymer Composites," *Poly. Compos.* **14(2)**, 101-115 (1993).
18. Wagner, H. D., Nairn, J. A., and Detassis, M., "Toughness of Interfaces from Initial Fiber-Matrix Debonding in a Single Fiber Composite Fragmentation Test," *Appl. Compos. Mat.* **2**, 107-117 (1995).
19. Moon, C. K., and McDonough, W. G., personal communication.
20. Matsuoka, S., Bair, H. E., Bearder, S. S., Kern, H. E., and Ryan, J. T., "Analysis of Non-linear Stress Relaxation in Polymeric Glasses," *Polym. Eng. & Sci.* **18(4)**, 1073-1080 (1978).

21. Christensen, R. M., *Theory of Viscoelasticity: An Introduction*, 2nd Ed., P 335 (Academic Press, New York, 1982).
22. Lai, J. S. Y., and Findley, W. N., "Stress Relaxation of Non-linear Viscoelastic Materials under Uniaxial Strain," *Transactions of the Society of Rheology* **12(2)**, 259-280 (1968).
23. Findley, W. N., Lai, J. S. Y., and Onoran, K., *Creep and Relaxation of Non-linear Viscoelastic Materials: with an Introduction to Linear Viscoelasticity*, pp. 229-233 (Dover Publications, Inc., New York, 1976).
24. Osaki, K., Proc. 7th International Congress on Rheology, Gothenburg, Sweden, 1976.
25. Laun, H. M., "Description of the Non-Linear Shear Behavior of a Low Density Polyethylene Melt of an Experimentally Determined Strain Dependent memory Function," *Rheologica Acta* **17(1)**, 1-15 (1978).